Journal of Structural Biology xxx (2009) xxx–xxx

Contents lists available at ScienceDirect

Journal of Structural Biology

journal homepage: www.elsevier.com/locate/yjsbi

Ultrastructure and mineral distribution in the tergal cuticle of the terrestrial isopod *Titanethes albus*. Adaptations to a karst cave biotope

Sabine Hild [a], Frank Neues [b], Nada Znidaršič [c], Jasna Štrus [c], Matthias Epple [b,*], Othmar Marti [d], Andreas Ziegler [a,*]

Q2 [a] Central Facility for Electron Microscopy, University of Ulm, Albert-Einstein-Allee 11, D89069 Ulm, Germany
[b] Institute of Inorganic Chemistry and Center for Nanointegration Duisburg-Essen (CeNIDE), University of Duisburg-Essen, Universitaetsstr. 5-7, 45117 Essen, Germany
[c] Department of Biology, University of Ljubljana, Večna Pot 111, SI-1000 Ljubljana, Slovenia
[d] Department of Experimental Physics, University of Ulm, Albert-Einstein-Allee 11, D89069 Ulm, Germany

ARTICLE INFO

Article history:
Received 17 April 2009
Received in revised form 17 July 2009
Accepted 18 July 2009
Available online xxxx

Keywords:
Amorphous calcium carbonate
Biomineralisation
Calcite
Cuticle
Isopoda
Titanethes
Cave

ABSTRACT

Composition and spatial distribution of organic and inorganic materials within the cuticle of isopods vary between species. These variations are related to the behaviour and habitat of the animal. The troglobiotic isopod *Titanethes albus* lives in the complete darkness of caves in the Slovenian Karst. This habitat provides constant temperature and saturated humidity throughout the year and inconsistent food supply. These conditions should have lead to functional adaptations of arthropod cuticles. However, studies on structure and composition of cave arthropod cuticles are rare and lacking for terrestrial isopods. We therefore analysed the tergite cuticle of *T. albus* using transmission and field-emission electron microscopy, confocal μ-Raman spectroscopic imaging, quantitative X-ray diffractometry, thermogravimetric analysis and atomic absorption spectroscopy. The ultrastructure of the epicuticle suggests a poor resistance against water loss. A weak interconnection between the organic and mineral phase within the endo- and exocuticle, a comparatively thin apical calcite layer, and almost lack of magnesium within the calcite crystal lattice suggest that the mechanical strength of the cuticle is low in the cave isopod. This may possibly be of advantage in maintaining high cuticle flexibility and reducing metabolic expenditures.

1. Introduction

Crustaceans have an exoskeleton, the cuticle, composed of an organic matrix containing chitin–protein fibrils and a mineral phase of mostly calcium carbonate. The cuticle serves as a support for organs and provides sites for muscle attachment. It protects the animal from internal and external mechanical stress and environmental hazards like desiccation and predation. Cuticular structures like scales and bristles are important in sensory orientation. Thus, depending on environmental stress, composition and structure of the crustacean cuticle vary to meet their functional purposes. During growth the cuticle has to be replaced by a new one in a process called moulting in which a new cuticular matrix has to be synthesised before, and mineralised after the old cuticle is shed. Although parts of the organic and sometimes inorganic components of the cuticle are resorbed before moulting (Greenaway, 1985) this process is very energy-consuming, requiring multiple steps of epithelial ion transport (Wheatly, 1999; Ziegler et al., 2005) and synthesis of organic molecules. Thus, in species adapted to the protected and relatively stable environment of caves, evolution may have led to a reduction of cuticle strength and rigidity.

The cuticle of isopods consists of four main layers, from distal to proximal: a thin unmineralised epicuticle, the mineralised exo- and endocuticles, and the unmineralised membranous layer (Price and Holdich, 1980; Štrus and Blejec, 2001). Wood and Russell (1987) first reported the amorphous character of the mineral phase in the cuticle of the terrestrial isopod *Oniscus asellus*. In addition to amorphous calcium carbonate (ACC), the mineral phase of the isopod cuticle consists of calcite that contains magnesium within its lattice (Mg-calcite) and amorphous calcium phosphate (ACP) (Becker et al., 2005; Neues et al., 2007a). Recent studies suggest that a similar composition is typical for many crustacean cuticles (Levi-Kalisman et al., 2002; Soejoko and Tjia, 2003; Boßelmann et al., 2007; Shechter et al., 2008a). For the terrestrial isopods *Porcellio scaber* and *Armadillidium vulgare* it was shown that Mg-calcite is restricted to the exocuticle, whereas the endocuticle contains ACC only together with magnesium and phosphate (Hild et al., 2008). Quantitative studies on the mineral phase of the intermoult cuticle of four marine and six terrestrial isopods have shown that the relative amounts of Mg-

Q3 * Corresponding authors. Fax: +49 (0) 731 50 23383 (A. Ziegler).
E-mail address: andreas.ziegler@uni-ulm.de (A. Ziegler).

1047-8477/$ - see front matter © 2009 Published by Elsevier Inc.
doi:10.1016/j.jsb.2009.07.017

calcite, ACC, and ACP vary considerably among species. The cuticles of marine isopods have a higher magnesium content and the variations in the Mg-calcite:ACC:ACP ratios is rather large compared to their terrestrial relatives, probably reflecting the high diversity in marine habitats. Terrestrial isopods have a lower magnesium content and there appears to be a consistent relation between cuticle composition and the animal's lifestyle (Neues et al., 2007a). Terrestrial isopods can be grouped into a number of categories that are related to ecological strategies and behavioural patterns (Schmalfuss, 1984). To avoid predation many isopods can roll into a perfect sphere, protecting their soft ventral body surface. These conglobating animals, the rollers, have short legs that can be hidden within the sphere together with the soft ventral regions of the exoskeleton relying on a hard and thick dorsal cuticle. These isopods walk slowly. The surface of the cuticle is smooth making it hard for a predator to break through the cuticle or to unroll the animal. Others cannot role into a sphere and have long legs. These isopods avoid predation by running away. The rather flexible cuticle of these runners is rather thin, and contains a high percentage of organic material and a low percentage of minerals. Members of a third group, the clingers, remain motionless for some time if they are suddenly disturbed, before they cling themselves to the substrate. They have a flat body, and their tight fitting of the epimera (the lateral ends of their tergites) make it difficult to detach the animal from the substrate. Most clingers have tubercles on the dorsal surface to increase the strength of the cuticle (Schmalfuss, 1984). Since clingers can still run away as a second option to escape a predator, little difference was found in the cuticle composition of runners and clingers. The cuticle composition of isopods representing other eco-morphological categories, like small-sized creepers and a number of "nonconformists" (Schmalfuss, 1984), has not yet been analysed.

With regard to evolutionary aspects of biomineralisation in terrestrial Crustacea, cave habitats may be of particular interest. Caves can provide conditions in which predation may be minimal providing little pressure to develop or maintain expensive protective functions within the exoskeleton during adaptation to cave biotopes. The troglobiotic isopod *Titanethes albus* lives in total darkness deep in the protected environment of caves in the karst of Slovenia and the northeastern Italy. The animals are quite large, about 2 cm in length, unpigmented, and eyeless (Fig. 1A). They probably orient themselves through tactile, chemical/olfactory, and possibly anemotactic stimuli like many other cave dwelling arthropods. The animals appear fragile and walk over the rocky and wet substrate (Fig. 1A), and sometimes go into the water. Throughout the year, they live at almost constant temperature and almost saturated relative humidity probably feeding on detritus.

In an attempt to further understand evolutionary aspects of biomineralisation we analysed the ultrastructure, spatial distribution, and composition of organic and inorganic components within the cuticle of *T. albus* employing transmission and field-emission scanning electron microscopy (TEM, FESEM), electron X-ray microprobe analysis (EPMA), scanning confocal μ-Raman spectroscopy (SCμ-RS), X-ray diffractometry (XRD), thermogravimetry (TG), and atomic absorption spectroscopy (AAS). Our results indicate that several characteristics of the cuticle of *T. albus* differ from that of other isopods. The outer epicuticle of *T. albus* apparently contains no lipid layers suggesting a poor resistance against water loss. A comparatively thin apical calcite layer, the virtual lack of magnesium within the calcite crystal lattice, and a weak interconnection between the organic and mineral phase suggest that the mechanical strength of the cuticle is rather low. These characteristics can be attributed to an evolutionary adaptation to the cave habitat.

2. Materials and methods

2.1. Animals

Titanethes albus (C. Koch, 1841) were collected from the Planina cave in central Slovenia. Specimens were collected from subterranean river bank and cave walls in spring 2005 and in spring 2007 and brought to the laboratory in cooled containers.

The animals were dissected in 100% methanol to avoid crystallisation of amorphous mineral phases. Previous studies have shown that amorphous calcium carbonate from sternal deposits of *P. scaber* is stable in methanol for at least 1 month (Becker et al., 2003). Tergites from the pereon and pleon were removed and any soft tissue was carefully cut away. Samples were washed for 1–2 s in double distilled water to remove tissue saline at the surface and then for 2–5 s in 100% methanol to remove water. Specimens were air dried and stored at −20 °C until further use. For Raman spectroscopic techniques and electron probe microanalysis pieces of air-dried tergites were glued onto plastic holders. Plain sagittal faces of cuticles were cut using an ultramicrotome (Reichert Ultracut) and glass knifes. These were then microtome-polished as described previously (Fabritius et al., 2005) using a diamond knife and by successively advancing the specimen 15 times each by 70, 40, 20, 10 and 5 nm.

2.2. Electron microscopy and electron microprobe analysis

For TEM analysis animals were injected with 12.5% glutaraldehyde in 0.1 M cacodylate buffer (Ziegler, 1997). Then tergites were isolated and fixed in 2.5% glutaraldehyde and 2% paraformaldehyde in 0.1 M cacodylate buffer (pH 7.3) overnight at 4 °C, and postfixed in 1% OsO_4 for 1 h. After washing and dehydration in a graded series of ethanol samples were embedded in Agar 100 resin. Ultrathin sections were contrasted with uranyl acetate and lead citrate, and examined with a CM 100 (Philips) transmission electron microscope. Images were documented with a 792 BioScan (Gatan) camera.

For SEM analysis cuticle samples were either cleaved in the sagittal plane, or sagittal surfaces were microtome-polished (see above) and sonicated in 100% methanol for 30 s or 15 min. Cleaved and microtome-polished/sonicated samples were rotary-shadowed with 3 nm platinum (BAF 100, Balzers) at an angle of 45°. SEM micrographs were recorded with a field-emission scanning electron microscopy (FESEM) (Hitachi S-5200) at an acceleration voltage of 10 kV. Electron probe microanalysis was performed with the same FESEM equipped with an EDAX (Phoenix) X-ray detector system with a 30-mm^2 SUTW window. For elemental analysis microtome-polished sagittal planes of tergites were washed briefly in 100% methanol and coated with a 10 nm thick film of carbon. Spectral maps (256 × 200 pixels) and lines scans (about 900 pixels) were recorded at an acceleration voltage of 20 kV at count rates between 1000 and 2000 s^{-1} using a dwell time of 500 ms/pixel and employing Genesis software (EDAX).

2.3. Raman spectroscopy

Single Raman spectra and Raman spectral images were recorded to localise calcite, ACC, and organic matrix within the tergite cuticle using a confocal Raman microscope (WITec, Ulm, Germany) equipped with an Nd-YAG laser (wavelength of 532 nm) and a Nikon 100× (NA = 0.95) objective. Purified chitin from crab-cuticle (Sigma–Aldrich) (VWR International) served as chitin standard. Pure calcite and ACC were synthesised as described in a previous publication (Hild et al., 2008) to obtain reference samples for spectral analysis of the tergite cuticle. Biogenic

Please cite this article in press as: Hild, S., et al. Ultrastructure and mineral distribution in the tergal cuticle of the terrestrial isopod *Titanethes albus*. Adaptations to a karst cave biotope. J. Struct. Biol. (2009), doi:10.1016/j.jsb.2009.07.017

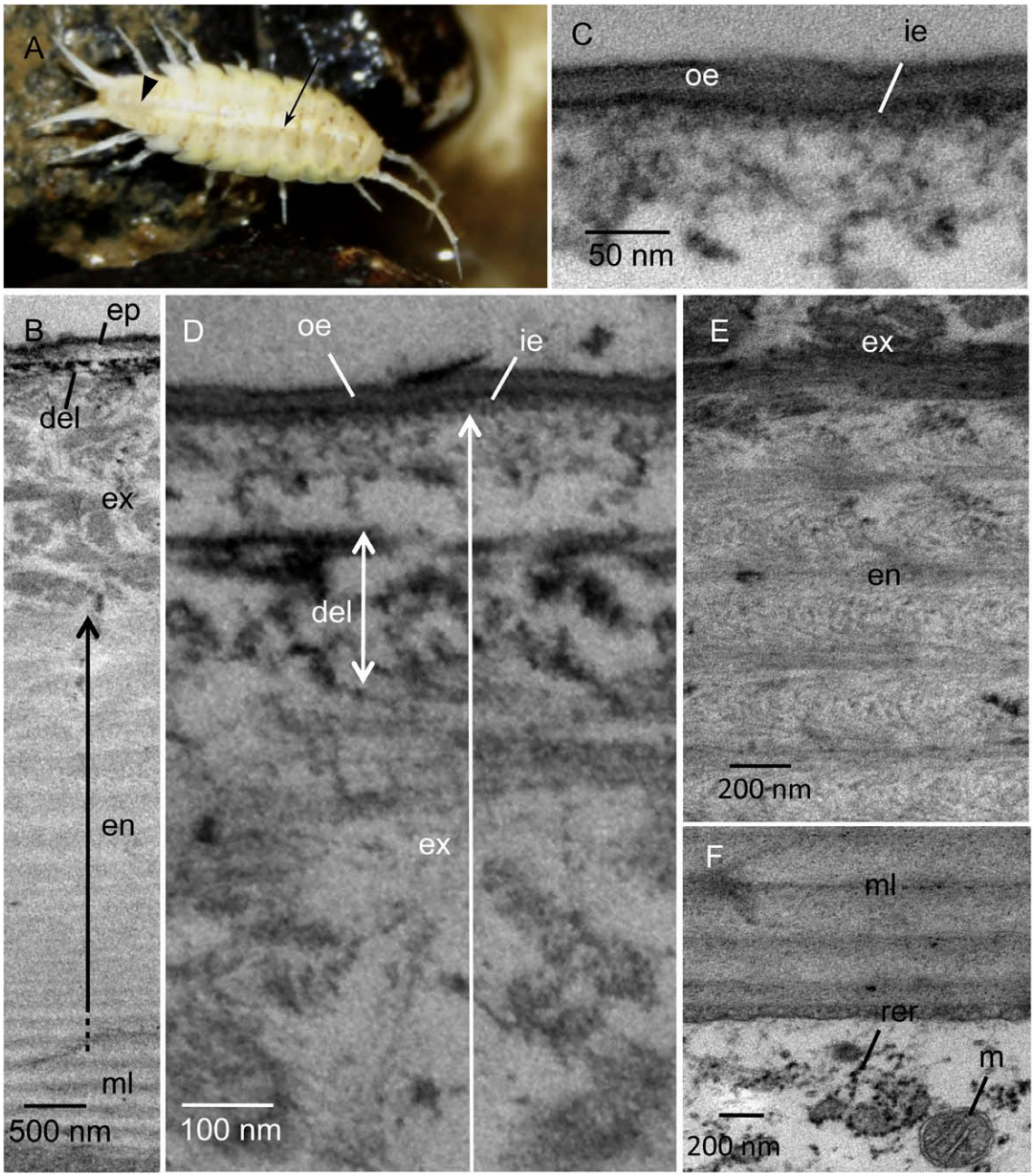

Fig. 1. (A) *Titanethes albus* in its natural habitat. Without appendages the animal measures about 15 mm in length. The arrow points to one of the seven tergites of the pereon the arrowhead to one of the pleon. (B–F) TEM micrographs of *T. albus* cuticle. (B) Overview of the tergite cuticle showing the main cuticular layers: epicuticle (ep), exocuticle (ex), endocuticle (en) and membranous layer (ml). A dense exocuticular layer (del) lies in a distal region of the exocuticle. (C) Detail of the distal cuticle showing the outer epicuticle (oe) the inner epicuticle (ie). (D) Distal part of the exocuticle and the epicuticle. (E) Detail of the endocuticle. (F) Detail of the membranous layer with subcuticular epithelial cell depicting rough endoplasmic reticulum (rer) and mitochondrium (m).

calcium phosphate was obtained from the pleoventral calcium phosphate deposits of *Tylos europaeus* (Ziegler, 2003). The Raman spectra of the standards were recorded with integration times of 250 ms and 5 s. To get high-resolution Raman spectra, microtome-polished sagittal surfaces of the cuticles (see above) were scanned while Raman spectra were recorded between 0 and 3750 cm^{-1} with integration times of 250 ms at every pixel (pixel density: 10 spectra at 1 μm). The overall Raman spectrum for a tergite cuticle of *T. albus* was obtained by averaging spectra collected along a 10 μm wide area across the polished surface of the sample. Raman spectral images were obtained analysing the integral of specific bands above background employing the WITecProject_1_86 software (WITec, Ulm, Germany) (Schmidt et al., 2005). All images were colour-coded: carbonate (orange), calcite (red) phosphate (blue) and organic material (green), glue (beige). Higher amounts of a specific component appear brighter.

2.4. X-ray powder diffractometry

For quantification of the calcite content per unit sample mass we mixed the cuticle samples with crystalline quartz (SiO_2) in a 5:1 = *w*:*w* ratio by thorough grinding. High-resolution X-ray powder diffractometry of the ground samples on Kapton foil was carried out at room temperature in transmission geometry at

beamline B2 at HASYLAB/DESY, Hamburg, Germany, at a wavelength of $\lambda = 0.70138$ Å (Knapp et al., 2004a,b). The data were converted to Cu Kα1 radiation wavelength ($\lambda = 1.54056$ Å) for better comparison with earlier results (Becker et al., 2005; Neues et al., 2007a,b). Quantitative Rietveld analysis was performed employing the software FULLPROF Suite 2005 (Rodriguez-Carvajal, 1990) which gave the relative mass fractions of calcite and quartz, the unit cell parameters and the reflex positions. The accuracy of this method is described in the literature (Gualtieri, 2000). Magnesium replacing calcium within the crystal lattice slightly changes the peak intensities and the phase scale factors during the Rietveld refinement. Furthermore, minor intensity shifts may occur due to the biological origin of the samples. Thus we estimated a relative error of about 5%. We used the method of Goldsmith (Goldsmith and Graf, 1958) to determine the amount of magnesium within the calcite lattice by analysing the decrease of the unit cell parameters *a* and *c*, and the shift of the position of the (1 0 4) reflex towards lower angles.

2.5. Thermogravimetric and elemental analysis

Thermogravimetric analysis (TG) was carried out with a Netzsch STA 409 PC instrument in dynamic oxygen atmosphere (50 mL min^{-1}). Samples were heated in open alumina crucibles to 1000 °C at a rate of 3 K min^{-1}. We assumed an error of about 0.5 wt.% for the thermogravimetric results (Cammenga and Epple, 1995). Total calcium and magnesium contents were quantified by atomic absorption spectroscopy (AAS) in a Unicam 939 instrument after extraction of calcium by suprapure HCl (average from two determinations). The maximum difference between two measurements was 1.0 wt.% for calcium and 0.01 wt.% for magnesium.

Calcium and magnesium concentrations in the water of subterranean Pivka river were determined by flame atomic absorption spectroscopy (FAAS, Varian SpectrAA 110, Mulgrave, Victoria, Australia) in three parallel determinations. Samples were transported to the laboratory within 2 h and kept in the refrigerator (<10 °C) until analysis.

3. Results

3.1. TEM analysis

The cuticle of the tergites is 6–10 μm thick (Fig. 1B). It consists of a distal epicuticle underlain by a 2–3 μm thick exocuticle, a 4–5 μm thick endocuticle and a proximal membranous layer varying in thickness between 0.5 and 1.5 μm. The epicuticle consists of an about 25 nm thick outer epicuticle and a thicker inner epicuticle (Fig. 1C and D). The three-layered outer epicuticle comprises thin outer and inner electron dense layers and a more lucent about 15 nm thick layer in between (Fig. 1C). The inner epicuticle has a granular appearance. Sublayers within the exocuticle, endocuticle, and the membranous layer are due to stacks of helicoidally arranged planar sheets of parallel chitin–protein fibres (Bouligand, 1972). In an about 150 nm thick distal region of the exocuticle organic fibres are more densely stained than in the main exocuticle (Fig. 1B and D). Distally to this dense layer the exocuticle contains spaces about 50 nm in size that are apparently devoid of organic material (Fig. 1C and D). The about 50 nm thick layer distally of these spaces may either belong to the exo- or inner epicuticle. In the exocuticle sublayers of helicoidally arranged sheets are 500–800 nm thick and the chitin–protein fibres are well visible. Within the endocuticle these sublayers are abundant and decrease in thickness from 300 nm to about 100 nm from the distal to proximal parts (Fig. 1B and E). The chitin–protein fibres are less stained as compared to the exocuticle. Pore canals are numerous extending through endo- and exocuticle. They are more prominent in the exocuticle than in the endocuticle. Within the membranous layer the sublayers are about 200 nm thick.

3.2. FESEM analysis

FESEM micrographs of the surface of sagittally cleaved tergites (Fig. 2A) indicate three different mineralised layers and one unmineralised most proximal layer, corresponding to the membranous layer, as indicated by the signal from the backscattered electrons (Fig. 2B). The most distal 40–50 nm thick layer possibly corresponds to the epicuticle (Fig. 2C). Below this layer, separated by a thin fissure, lies a strongly mineralised 500–700 nm thick layer, which belongs to the exocuticle. In this region the surface of sagittally cleaved cuticle appears smooth and composed of tightly arranged granules 10–20 nm in diameter (Fig. 2C and the insert in Fig. 2E). There is no spatial correlation of the smooth layer with any distinct sublayer apparent in TEM images. Proximally of the smooth layer the exocuticle appears rough and composed of interconnected aggregates leaving large voids between them (Fig. 2A and D). At least some of the voids are probably related to the pore canals. Voids and pore canals become particularly apparent in knife-polished samples that were sonicated in 100% methanol for 15 min (Fig. 2E). Sublayers due to helicoidally arranged plains of parallel chitin–protein fibres are poorly defined within the exocuticle, but can be well recognised within the endocuticle and membranous layer (Fig. 2A and E). In the endocuticle large voids are lacking and pore canals can be well recognised (Fig. 2A and E). In both the proximal part of the exocuticle and the endocuticle mineral occurs in irregularly distributed granular substructures with diameters between 10 and 20 nm (Fig. 2F and G). Chitin–protein fibres with diameters between 10 and 15 nm stick out of cleaved surfaces and are devoid of mineral granules (Fig. 2F and G). Within the endocuticle numerous chitin–protein fibres that are devoid of mineral granules can be observed. Even in knife-polished exo- and endocuticle sonicated for 30 s no spatial correlation between the distribution of mineral granules and chitin–protein fibres is visible (Fig. 2H). Large numbers of these fibres are observable in the cleaved membranous layer (Fig. 2I).

3.3. Elemental distribution (EPMA)

Elemental maps of sagittal surfaces of the mineralised cuticle are shown in Fig. 3. X-ray spectra of the cuticles show the presence of carbon, oxygen, phosphorus, and calcium (Fig. 3A). In addition, there is a small peak for sodium, probably originating from salts in extracellular body fluids, and a marginal peak for magnesium that indicates a very low concentration within this species (see also the AAS measurements below). Elemental maps and line scans show that high calcium signals extend from the distal edge to about four fifths of the cuticle thickness. There it is decreasing by about 20% before it decreases towards the unmineralised membranous layer (Fig. 3B). The elemental map for the low amounts of magnesium shows that magnesium is not concentrated to any specific sites within the cuticle (Fig. 3C). The phosphorus content is low in the distal first tenth of the cuticle and increases towards a plateau that covers the next four tenths of the cuticle thickness (Fig. 3D). From the middle of the cuticle towards the membranous layer the phosphorus content declines. The membranous layer contains only little phosphorus.

3.4. Raman imaging

Raman spectra of standards are shown in Fig. 4A, a–d. Bands in the range of 2800–3200 cm^{-1} in the chitin standard (Fig. 4A, 1) can be assigned to CH-stretching vibrations. The double band (Fig. 4A,

Please cite this article in press as: Hild, S., et al. Ultrastructure and mineral distribution in the tergal cuticle of the terrestrial isopod *Titanethes albus*. Adaptations to a karst cave biotope. J. Struct. Biol. (2009), doi:10.1016/j.jsb.2009.07.017

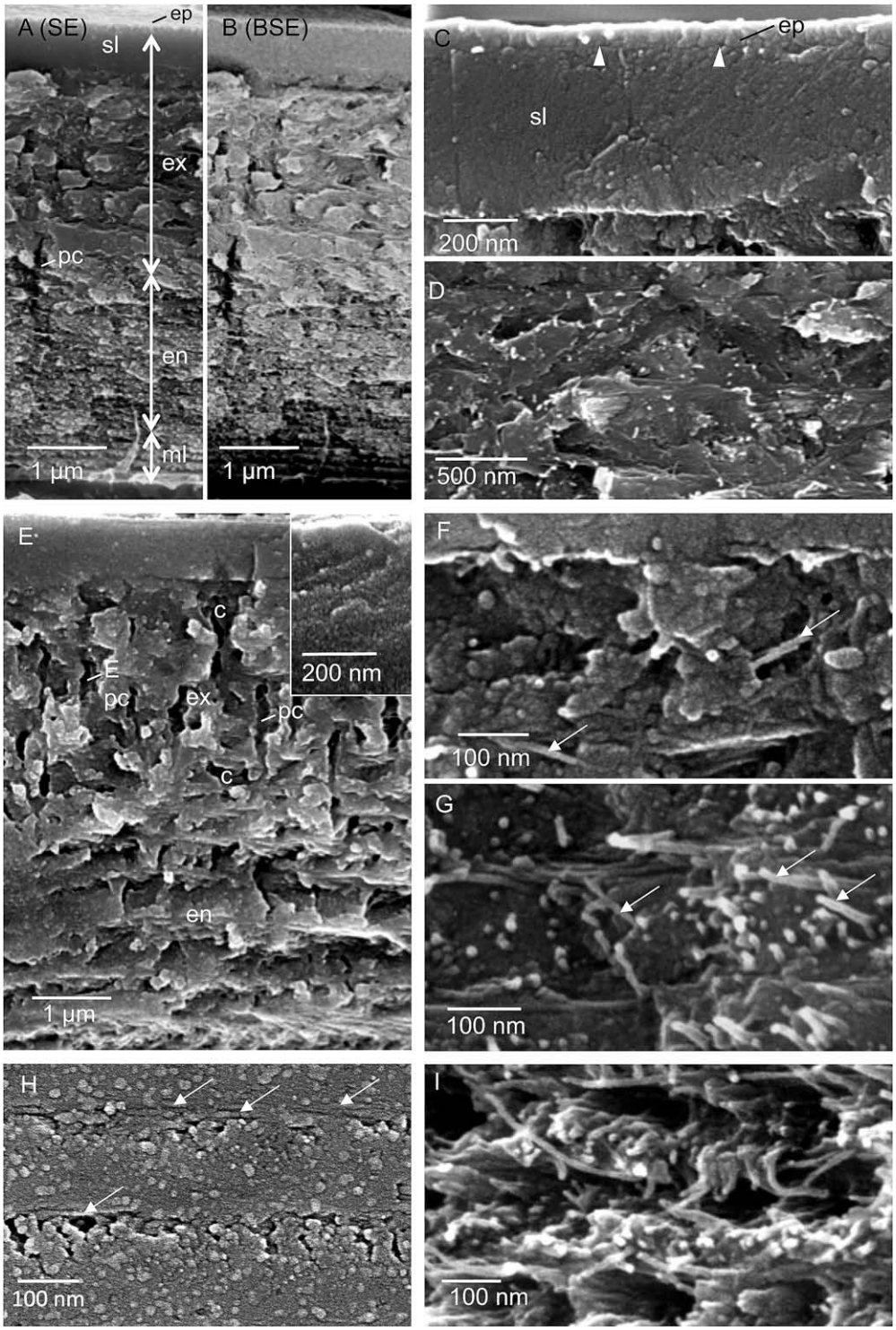

Fig. 2. Field-emission scanning electron microscopy of sagittally cleaved mineralised tergite cuticle of *Titanethes albus*. (A) Overview showing the principal layers of the cuticle using secondary electron detector (SE): the cuticle consists of a thin distal epicuticle (ep), a mineralised exocuticle (ex) comprising a distal layer of smooth appearance (sl), a proximal part containing pore channels (pc), a mineralised endocuticle (en) and a unmineralised membranous layer (ml). (B) Same as "(A)" but using a backscatter electron detector (BSE). Regions containing mineral appear bright. (C) High-resolution image of the smooth layer. A thin fissure (arrowheads) separate epicuticle and smooth layer. (D) Micrograph of the exocuticle just below the smooth layer (E). Knife-polished sample sonicated for 15 min in 100% methanol revealing large number of pore channels and caverns (c). The insert provides a high-resolution image of the smooth layer revealing a granular texture. (F–I) High-resolution micrographs of the exocuticle (F), cleaved (G) and knife-polished (H) samples of the endocuticle, and membranous layer (I). Chitin protein fibres (arrows) appear devoid of mineral granules.

2) with maxima at 3275 cm^{-1} and 3450 cm^{-1}, respectively, is characteristic for amide and hydrogen bonds present in chitin (Galat and Popowicz, 1978). Both calcite and ACC standards (Fig. 4A, b and c) show bands assigned to carbonate stretching vibrations (Fig. 4A, 3) having their maxima at 1086 cm^{-1} and 1080 cm^{-1}, respectively. Calcite can be discriminated from ACC by distinct lattice vibrations at 158 cm^{-1} and 280 cm^{-1} (Fig. 4A, 4) (Rutt and Nicola, 1974). In ACC these two peaks are replaced by a single broad band ranging from 100 to 300 cm^{-1} (Fig. 4A, 5) (Tlili et al., 2001). The calcium phosphate spectrum (Fig. 4A, d) is dominated by a

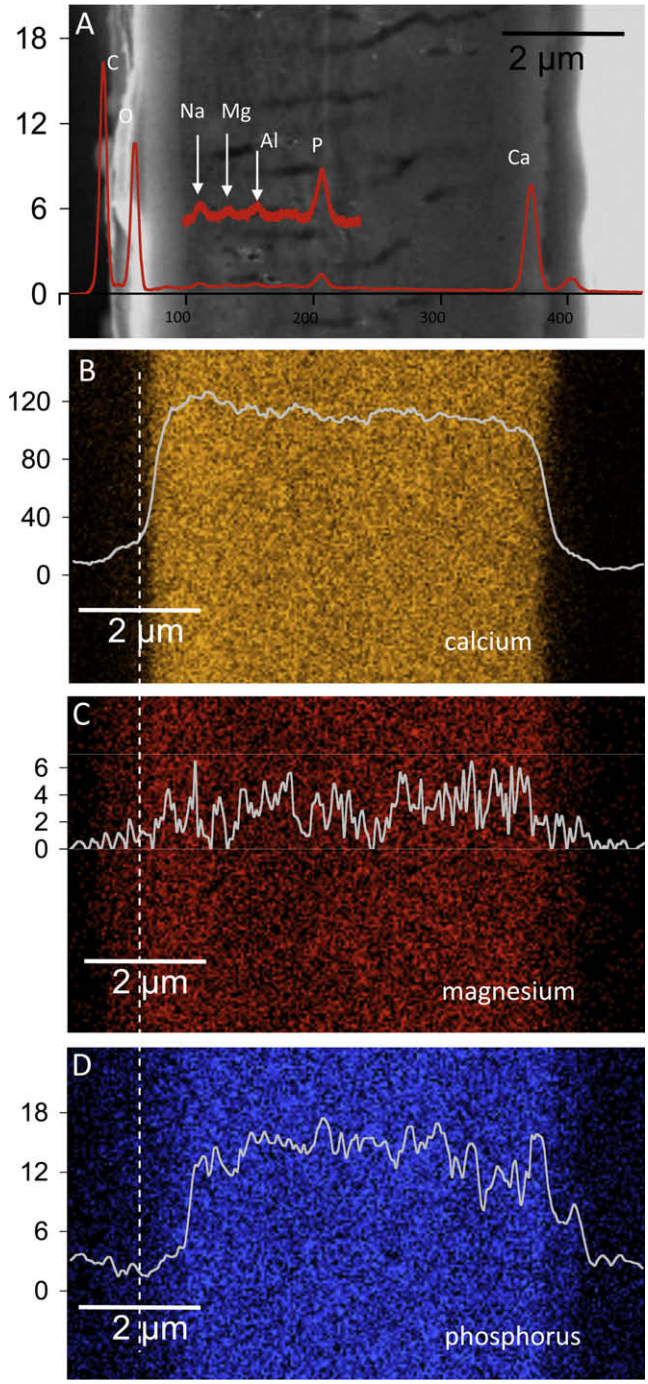

Fig. 3. Electron probe microanalysis of sagittally cleaved and microtome-polished surfaces of the mineralised tergite cuticle of *Titanethes albus*. (A) SEM image and elemental X-ray spectrum indicate the presence of C, O Na, Mg, P and Ca. The aluminium peak is due to the conductive glue at the sides of the specimen. Spectral maps and line scans are given for calcium (B), magnesium (C) and phosphorus (D).

strong band at around 960 cm^{-1} that derives from the symmetric stretching mode of the phosphate group. The exact position of this band varied slightly among the different mineral standards, ranging from 952 cm^{-1} for amorphous calcium phosphate, to 957 cm^{-1} for octacalcium phosphate, and up to 960 cm^{-1} for hydroxyapatite (Sauer et al., 1994). In case of the recorded biogenic phosphate the band (Fig. 4A, 6) appears with its maximum at 958 cm^{-1} that strongly points to octacalcium phosphate. The presence of a broad, weak HPO_4 band with a maximum at about 420 cm^{-1} as well as the configuration of a PO_4 band at 590 cm^{-1} (Fig. 4A, 7) (Sauer et al., 1994) supports this assumption.

The averaged Raman spectrum for the tergite cuticle of *T. albus* (Fig. 4B, a) shows bands ranging from 2800 to 3100 cm^{-1} characteristic for the organic matrix. The double band in the range from 3100 to 3300 cm^{-1} indicates the formation of a chitin-based organic matrix that is reinforced by calcium carbonate. The presence of amorphous and crystalline calcium carbonate is indicated by a band at 1080 cm^{-1} and a band ranging from 100 to 300 cm^{-1}, which has an additional maximum at 280 cm^{-1}. After subtracting the chitin spectrum (Fig. 4B, b) the inorganic components can be seen more clearly. In enlargement of the region up to 1050 cm^{-1}, besides the bands characteristic for ACC and calcite, a small band appearing in the range of 950–970 cm^{-1} indicates the presence of inorganic phosphate.

To obtain Raman spectral images of the distribution of total calcium carbonate the integral values of the spectral area ranging from 1070 to 1100 cm^{-1} (Fig. 4B, a), that includes the carbonate band, were recorded and plotted in *x–y* coordinates. The resulting Raman spectroscopic images indicate that calcium carbonate occurs within the whole exo- and endocuticle (Fig. 5A). The inner membranous layer appears to be virtually devoid of calcium carbonate. Plotting the integral values of the spectral area-range from 200 to 300 cm^{-1} corresponding to the calcite lattice vibration at 280 cm^{-1} (Fig. 4B, b) reveals the local distribution of calcite only (Fig. 5B). Apparently, calcite is restricted to the distal tenth of the cuticle. Raman spectral line scans (Fig. 5E) allowed a more detailed analysis. The carbonate signal is particularly strong within the distal 1.5 µm of the cuticle, corresponding to the distribution of calcite. Proximally the signal decreases to about one third of the maximum intensity and no significant change can be found within the next 6–7 µm. Towards the membranous layer the signal decreases to the background level. From single Raman spectra taken within the region of the highest carbonate signal (Fig. 5F, a) it can be concluded that mainly calcite is present there, whereas the region with medium signal contains both calcite and ACC. The domains with the highest calcium signal can be correlated with the distal layers of the exocuticle. This leads to the conclusion that the distal region of the exocuticle contains both ACC and calcite whereas only ACC is present within the proximal layers of the exocuticle and the endocuticle (Fig. 5E). Plotting the intensity of the integral values of the phosphate band (Fig. 4B and C) reveals the absence of phosphate in the region with highest calcite content but its spatial correlation with ACC and some overlap with a proximal region containing no ACC. This overlap may be due to inorganic phosphate either within the membranous layer or a proximal layer of the endocuticle that is devoid of ACC.

3.5. Content of water, calcium carbonate and organic material

An overview of all quantitative values obtained by XRD, TG and AAS is presented in Table 1. Weight fractions are given with respect to the sample mass still containing residual water. The formulae for all calculations are described in detail elsewhere (Becker et al., 2005). For the determination of the content of calcite and ACC we used a combination of elemental analysis and X-ray powder diffractometry. The total contents of calcium and magnesium were 24.5 and 0.17 wt.%, respectively, as determined by atomic absorption spectroscopy. The contents of water, organic matrix and calcium carbonate were obtained by TG analysis (Fig. 6). During the first TG step from 50 to 210 °C the sample mass decreased by 7.6 wt.% due to the loss of adsorbed or incorporated water still present after methanol treatment and air drying. The mass loss from 210 to 550 °C is due to combustion of 24 wt.% organic material. The decrease in mass between 550 and 680 °C is due to release of carbon dioxide after decarboxylation of calcium

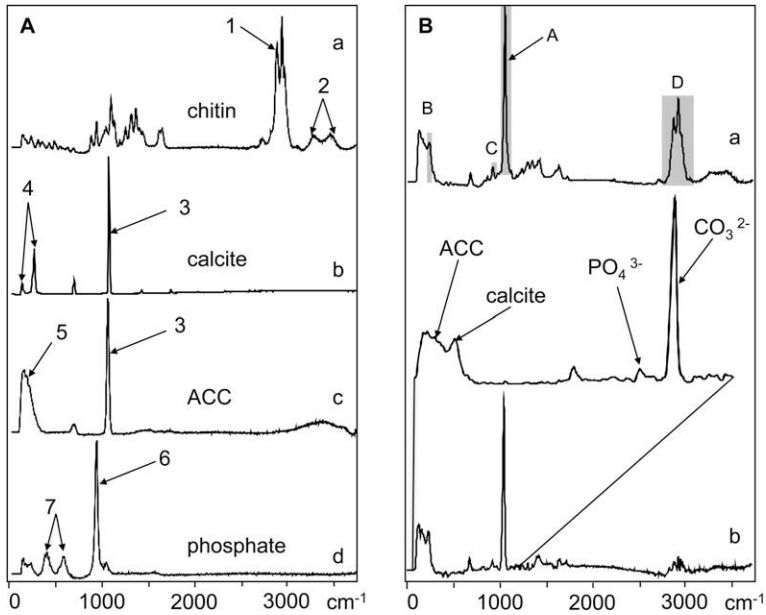

Fig. 4. In the reference spectra (A) for the Raman analysis specific bands for chitin (a), calcite (b), amorphous calcium carbonate (ACC) (c) and phosphate (d) are marked by the numbers 1–7. The averaged spectrum recorded from a sagittally cleaved and microtome-polished surface of the tergite cuticle of *Titanethes albus* is normalised to the organic peak ranging from 2500 to 3200 cm^{-1} (B, a). After subtraction of the normalised chitin spectrum only inorganic components appear (b). Bands (A–D) integrated to obtain Raman spectroscopic images marked in the averaged spectrum (a).

carbonate. From the latter, a content of 52.1 wt.% calcium carbonate in the cuticle was calculated by stoichiometry, assuming that all carbon dioxide originated from calcium carbonate. To determine the amount of calcite within the cuticle we used X-ray powder diffractometry of samples containing the tergite cuticle mixed with defined amounts of SiO_2. The ratio of the two compounds was obtained from Rietveld refinement of the X-ray powder diffractogram (Fig. 7). From the known mass of the quartz standard an amount of 9.6 wt.% of crystalline Mg-calcite in the cuticle was calculated. The difference of 42.5 wt.% between the amount of total calcium carbonate calculated from the CO_2 release during TG, and the amount of crystalline calcite obtained by Rietveld refinement corresponds to ACC. Analysing the shift in calcite reflex positions and the change of the unit cell parameters a and c from X-ray diffractograms (Goldsmith and Graf, 1958) revealed that the amount of Mg within Mg-calcite was below 0.01 wt.%. A second X-ray powder diffractogram (Fig. 8) obtained from the cuticle after the TG experiment and thus heating the sample to 1000 °C showed peaks of hydroxyapatite ($Ca_5(PO_4)_3OH$ (HAP). Here, the expected reflections for calcium oxide (CaO), and magnesium oxide (MgO) were missing. Instead, due to rehydration of calcium oxide after cooling, peaks of calcium hydroxide were present. Since HAP reflections were absent from the initial diffractogram we conclude that calcium phosphate was present within the native cuticle in amorphous form (ACP), which was apparently transformed into hydroxyapatite by heating. Assuming that ACP has the same stoichiometry as HAP (Becker et al., 2005), we indirectly computed the amount of 9.1 wt.% ACP from the difference between the total calcium content within the cuticle determined by AAS and the amount of calcium within calcite as obtained from TG.

3.6. Calcium and magnesium content in cave river water

Water samples from the subterranean river of the Planina cave sampled in the first three consecutive months of the year 2009 had calcium and magnesium concentrations of 1.55 ± 0.05 and 0.148 ± 0.004 mmol L^{-1}, 1.57 ± 0.05 and 0.181 ± 0.004 mmol L^{-1}, and 1.77 ± 0.05 and 0.181 ± 0.004 mmol L^{-1}, respectively.

4. Discussion

4.1. The structure of the tergite cuticle

The tergite cuticle of *T. albus* consists of the same principal layers as described in most crustaceans including other terrestrial isopods (Price and Holdich, 1980; Ziegler, 1997; Glötzner and Ziegler, 2000; Štrus and Blejec, 2001). Structure and thickness of the outer epicuticle correspond to the cuticulin layer described for terrestrial isopods (Compère, 1990) in analogy to that described in insects (Locke, 1966) and decapod crustaceans (Compère, 1995). A cement layer and a surface coat, which cover the cuticulin layer, and the waxy layer that lies within the cuticulin layer as described in *O. asellus* (Compère, 1990) are lacking in *T. albus*. The cement and the waxy layers are not present in marine crustaceans and are, therefore, assumed to be adaptations to the terrestrial environment. In particular the lipids and waxes within the outer cuticle of terrestrial isopods are thought to be the main barriers for evaporative water loss (Hadley and Warburg, 1986; Compère, 1990). Thus the lack of the waxy layer in *T. albus* is likely to be an adaptation to the saturated humidity of its cave habitat. This interpretation is in accordance with a greater integumental permeability and smaller quantities of lipids extracted from the epicuticle of troglobiotic insects and spiders living in Hawaiian lava tube caves and in Laurel Cave, Carter Co., KY, as compared to their epigean relatives (Hadley et al., 1981; Ahearn and Howarth, 1982; Yoder et al., 2002).

We cannot provide any reason for the absence of the cement layer and surface coat in *T. albus*. The surface coat in the gill cuticle of *Carcinus maenas* contains glycoproteins and acid mucopolysaccharides (Compère and Goffinet, 1995). Such a hydrophilic external sublayer is thought to be a general feature of aquatic arthropods, and it may function in protecting and/or reducing the surface tension between the hydrophobic cuticulin layer and the aquatic environment (see Compère and Goffinet, 1995, for further discussions). A surface coat is also present in the terrestrial isopod *O. asellus*, but appears to be much thinner than in marine crustaceans (Compère, 1990).

Please cite this article in press as: Hild, S., et al. Ultrastructure and mineral distribution in the tergal cuticle of the terrestrial isopod *Titanethes albus*. Adaptations to a karst cave biotope. J. Struct. Biol. (2009), doi:10.1016/j.jsb.2009.07.017

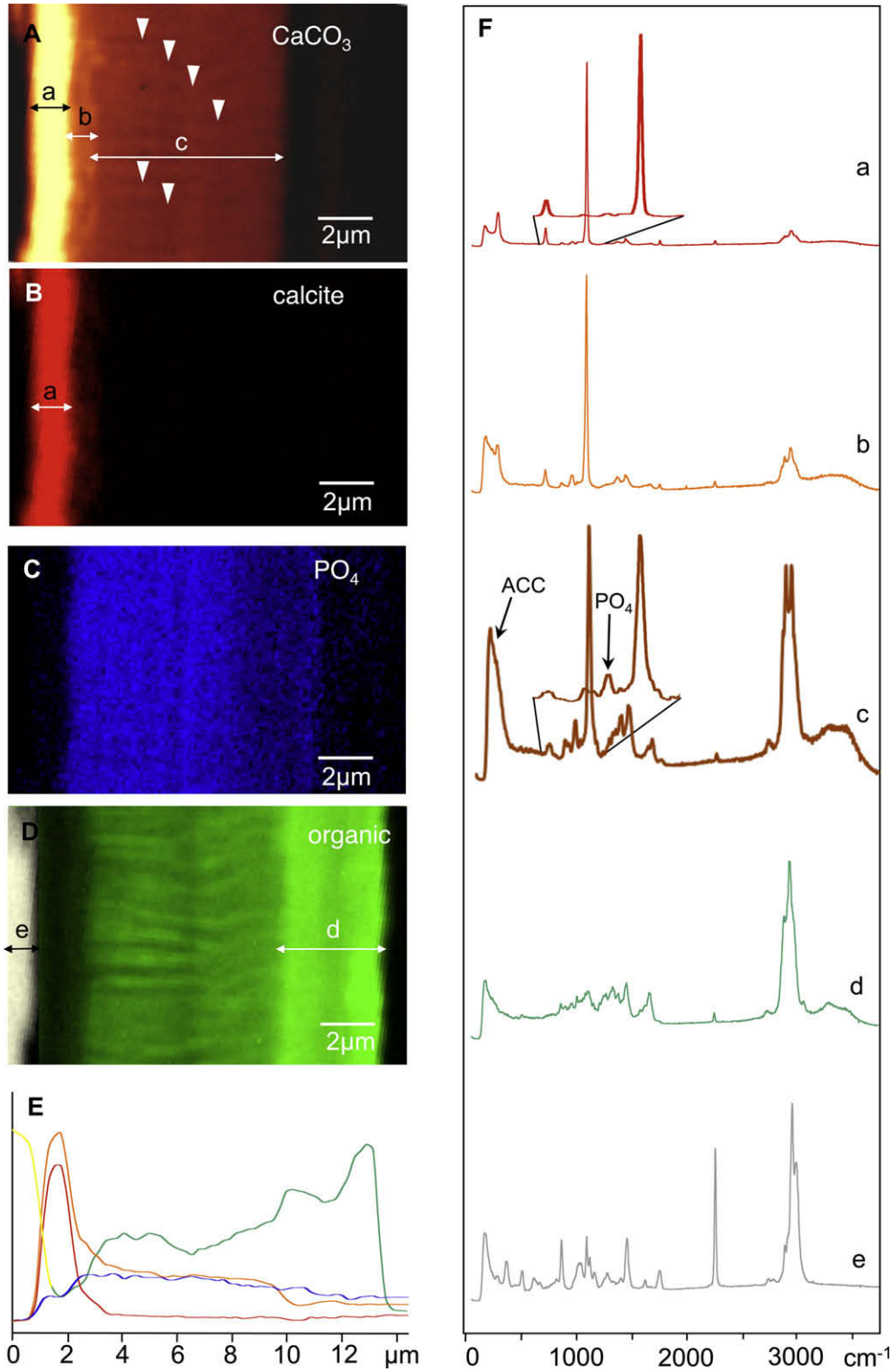

Fig. 5. Raman spectroscopic images (A–D), line scans (E) and cumulated spectra (F) recorded from a sagittally cleaved and microtome-polished surface of the tergite cuticle of *Titanethes albus*. Calcite is located in a distal layer (a) of the exocuticle (A and E) and to a much lesser extent within a region (b) just proximal of the calcite-containing layer (B and E), whereas calcium carbonate occurs within the whole exo- and endocuticle (b and c), the membranous layer is devoid of mineral (B and E). Phosphate is scarce in the distal calcite layer, whereas the mineralised layer proximally of the calcite layer contains significant amounts of phosphate that decreases towards the membranous layer (C and E). (D) The signal for the organic matrix is low in the calcite-containing layer, intermediate within the proximal part of the exocuticle and within the endocuticle, and highest within the membraneous layer. The organic material at the distal side of the cuticle (e) originates from the superglue (D and F). Double arrows in the images A, B and D labelled with a–d indicate the areas from which cumulated spectra (F) were recorded. Capital letters in (F) indicate the band areas used for the chemical maps A–D. Arrows (pore cannels).

The mechanical strength of the cuticle of *T. albus* appears to be comparatively low. It broke easily during dissection and is very thin (10 µm) for a rather large animal (20 mm). For comparison, the cuticle of the strictly terrestrial isopods *P. scaber* is about twice

Table 1
Composition of the tergite cuticle of *Titanethes albus* (in wt.% if no other unit is given). ACP was computed as hydroxyapatite. The column "total mass" denotes the sum of Mg-calcite, ACC, organic matrix and ACP.

Ca (AAS)	Mg (AAS)	Water (TG)	Organic matrix (TG)	Total mineral content (TG)	$CaCO_3$ (TG)	Crystalline Mg-calcite (XRD)	ACC (XRD and TG)
24.5	0.17	7.6	24.0	68.3	52.1	9.6	42.5
ACC/calcite (wt.%:wt.%)	Mg/Ca (wt.%:wt.%)	$MgCO_3$ in Mg-calcite (mol%)	Mg in Mg-calcite	Mg not in Mg-calcite	Ca not in $CaCO_3$	ACP	Total mass
4.40	<0.01	0.19	<0.01	0.16	3.6	9.1	93.0

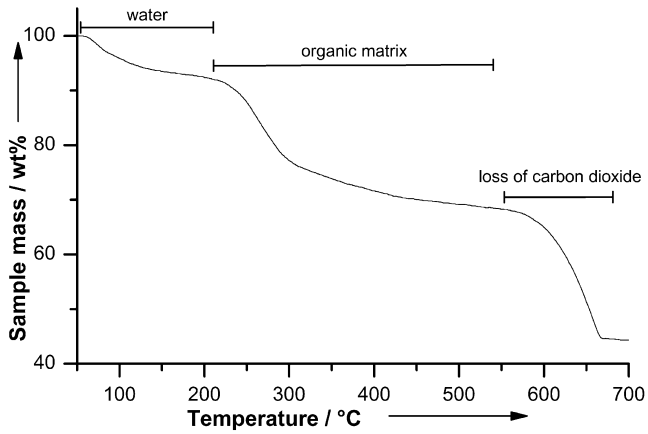

Fig. 6. Thermogravimetry of the cuticles of *Titanethes albus*. The weight loss can be assigned to three steps: loss of water (from 60 to 200 °C), combustion of organic material (from 200 to 560 °C), and decarboxylation of calcium carbonate (from 560 to 680 °C).

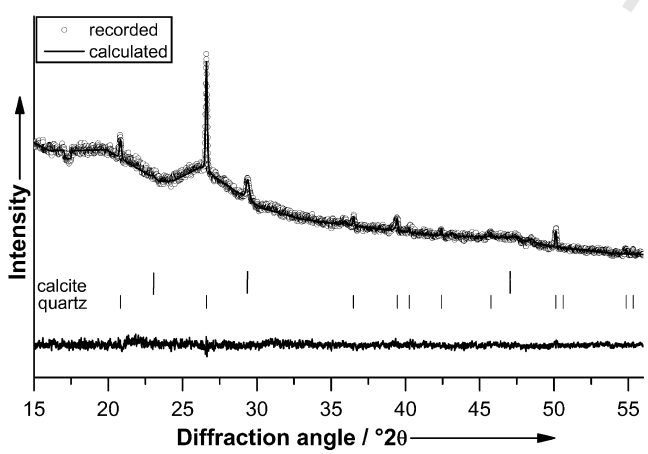

Fig. 7. Rietveld plot of the cuticle of *Titanethes albus*, mixed 5:1 with quartz. The upper graph shows the recorded data and the calculated data (fit results). At the bottom, the difference curve between observed and calculated intensity is shown. In addition, the calculated peak positions for calcite and quartz are shown.

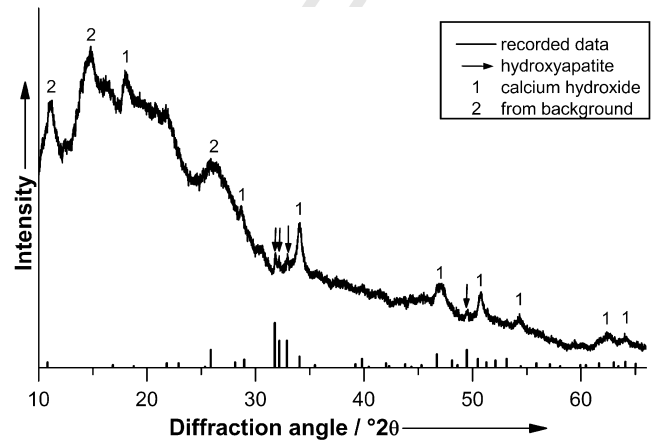

Fig. 8. X-ray powder diffractometry of the mineralised cuticle of *Titanethes albus*, (after thermogravimetry to 1000 °C). The computed positions for hydroxyapatite (HAP) are shown at the bottom and the arrows mark the corresponding signals. Signals from calcium hydroxide (1) and those from the background (2) are marked by numbers. Calcium hydroxide results from rehydration of calcium oxide after cooling.

as thick and that of the conglobating *A. vulgare* can be even four times thicker (Hild et al., 2008), although both animals are smaller than *T. albus*. The cuticle of *Ligidium hypnorum* that is only 5–6 mm long, and adapted to living in moist surface habitats, has about the same thickness as that of *T. albus*. It was suggested that cuticle thinning is a common troglomorphic characteristic (Christiansen, 2004). For example, the cuticle of the cave cricket *Hadenoecus subterraneus* is half as thick as the cuticle of the *Centhophilus stygius* which uses the cave environment only as daily refuge (Lavoie et al., 2007). *T. albus* has a rather slender shape of the body and long legs. The length of legs and body appendages is characteristic for troglobionts and is thought to facilitates reception and orientation. In addition long legs help to walk fast and facilitate walking over substrates of rough topology like gravel, mud, and rock that contain many crevices. With regard to the eco-morphological strategies established by Schmalfuss (1984, see the Introduction for a short survey) the slender shape of the body and length of the legs would raise the possibility that *T. albus* avoids predation by running away rather then clinging to the substrate. This would also make a robust exoskeleton dispensable. Similarly, lack of any significant predation could also explain a thin cuticle. Although there are several potential predators such as beetles, spiders, leeches and bats there is little information regarding predation on *T. albus*. More knowledge on the ecology of troglobiotic isopods would be required to establish the relation between mechanical properties of the *T. albus* cuticle and predation.

A schematic overview of the composition of *T. albus* tergite cuticle in its dry state is provided in Fig. 9. Comparison of the relative content of organic matrix and calcium carbonate with that of other isopods shows that the overall composition of *T. albus* is similar to that of runners or clingers which contain 22–27 wt.% organic matrix and between 44 and 63 wt.% calcium carbonate, whereas rollers have a lower amount of organic material (13–16 wt.%) and more calcium carbonate (71–75 wt.%) (Neues et al., 2007a). However, the cuticle of *T. albus* differs from that of the runners and clingers by a significant lower relative content of calcite. Furthermore, the calcite-containing layer in *T. albus* covers only one tenth of the cuticle thickness and is restricted to a distal part of the exocuticle, whereas in *A. vulgare* and *P. scaber* the whole exocuticle contains calcite and covers one fifth of the cuticle (Hild et al., 2008). Preliminary experiments on isopod cuticular layers using a nanoindenter indicate that calcite-containing layers are harder than layers containing ACC (Hild, unpublished). Thus it may be concluded that, perhaps due to lesser mechanical strains in a cave environ-

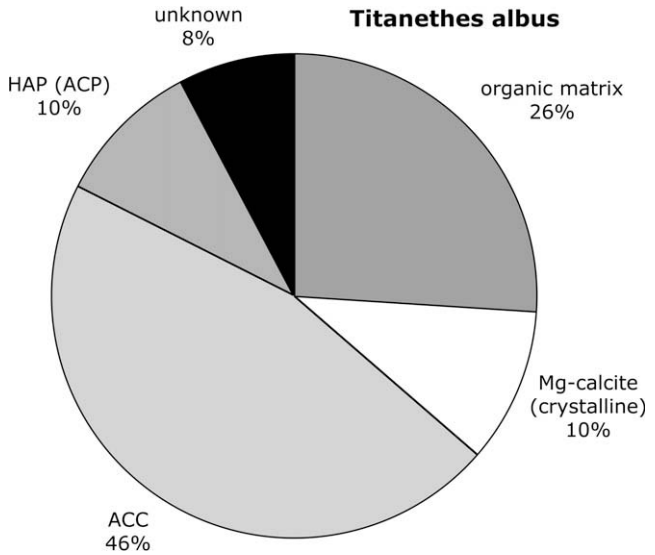

Fig. 9. Schematic overview of the mineral composition in the dry state of the tergite cuticle of *Titanethes albus*.

ment, part of the mechanical strength of the cuticle was lost, possibly in favour of a higher flexibility that might be useful when foraging for esculent detritus within small crevices. In *P. scaber and A. vulgare* as well as in other crustaceans, cuticular calcium carbonate occurs as calcite and ACC in the form of nano-granules that are aligned along the protein–chitin fibres (Roer and Dillaman, 1984; Dillaman et al., 2005; Boßelmann et al., 2007; Hild et al., 2008). This indicates a strong connection between mineral and organic fibres that is responsible for the excellent mechanical properties of the cuticular composite material. The association between mineral and protein–chitin fibres appears to be much weaker in *T. albus* as indicated by the high-resolution FESEM images of knife-polished surfaces and the smooth appearance of protein–chitin fibres that stick out of cleaved surfaces. It is likely that a weak connection between mineral and organic phase leads to a decrease in mechanical strength of the composite.

Within the terrestrial isopods studied so far (Becker et al., 2005; Neues et al., 2007a) *T. albus* has the lowest magnesium content within the cuticle and the lowest amount of magnesium in Mg-calcite. Marine isopods that have ready access to the magnesium in seawater have a much higher percentage of magnesium within their cuticle than terrestrial isopods, suggesting that abundance of magnesium within the animals environment is an important factor for the magnesium content within the cuticle (Neues et al., 2007a). The magnesium concentration within the Planina cave river, however, is within the range of magnesium concentration known from epigean rivers (Hem, 1985). Therefore, it appears unlikely that the difference in cuticle magnesium between *T. albus* and epigean isopods is due to differences in environmental magnesium. Mg-calcite may also be formed for functional reasons as discussed previously (Becker et al., 2005). Calcite-containing magnesium within the crystal lattice is harder than calcite without magnesium. Thus, in *T. albus* high amounts of magnesium within the cuticle may be disadvantageous. Possible explanations are that magnesium could affect the flexibility of the cuticle, or that in the cave habitat of *T. albus* the benefits of having a harder cuticle do not compensate the disadvantage of the energy costs arising from the incorporation of magnesium into the cuticle. Studies on the metabolic relations in cave adapted and epigean arthropods have shown that the metabolic activity can be considerably lower in the troglobiotic species (Hadley et al., 1981; Hueppop, 1985), possibly an adaptation to inconsistent food supply (Anderson, 1970) and/or lack of predators (Hueppop, 1985). However, the metabolic rate is not universally reduced in subterranean species and metabolic rates are thought to be related to the energy state of a hypogean system (Mejía-Ortíz and López-Mejía, 2005). In *T. albus* rare moulting and reproductive events point to metabolic stress, probably due to irregular supply of energy into the Slovenian Karst system by unpredictable flushes of surface water.

The correlation of the phosphorus and phosphate distribution with that of ACC as shown in the present study by EDX and Raman spectroscopic analysis, respectively, and the indirect demonstration of ACP by X-ray diffraction analysis suggests that the endocuticle contains ACP. Furthermore, it suggests that possibly phosphate contributes to ACC stabilisation during mineralisation of the tergite cuticle of *T. albus*. In vitro experiments have shown that magnesium and phosphate support ACC formation during mineral precipitation (Bachra et al., 1963; Reddy, 1977; Aizenberg et al., 2002; Loste et al., 2003). In fact the ACC in the cuticle of most isopods contains both phosphate and magnesium (Becker et al., 2005; Neues et al., 2007a; Hild et al., 2008), however, it is unknown whether these ions stabilize ACC in vivo. Furthermore, it is known that proteins play a role in the regulation of mineral deposition and in the stabilisation of ACC (Shafer et al., 1995; Coblentz et al., 1998; Fabritius and Ziegler, 2003; Luquet and Marin, 2004; Sugawara et al., 2006; Shechter et al., 2008b). The very low magnesium content within both calcite and ACC of the cuticle of *T. albus* indicates that magnesium is not essential for ACC formation. This is supported by the recent observation that in the cuticle of *P. scaber* and *A. vulgare* (Hild et al., 2008) and of *Homarus americanus* (Al-Swalmih et al., in press), that contain significant amounts of both magnesium and phosphorus, the distribution of phosphorus but not of magnesium correlates with that of ACC. This suggests that phosphate rather than magnesium may play a role in ACC formation. However, the presence of phosphate appears not to be essential for ACC formation in the terrestrial species *Armadillo officinalis* and the marine isopod *Spheroma serratum* in which phosphate is virtually absent from the cuticle (Neues et al., 2007a). Because of the vast variation in the distribution of phosphate and magnesium ions and their sometimes very low concentrations it remains unclear if these ions have a general function in the stabilisation of biogenic ACC. In contrast, the role of specific proteins in ACC stabilisation appears well established. If inorganic ions can enhance stabilisation of ACC in the presence of specific proteins and/or other organic components remains to be established.

5. Uncited reference

Ziegler (1994). Q1

Acknowledgments

We like to thank Rok Kostanjsek for collecting animals and providing the photographs of the animals and Magda-Tusek Znidaric for technical assistance regarding TEM preparation. This work was supported by the Deutsche Forschungsgemeinschaft, within the priority program "Principles of Biomineralisation" (SPP 1117, Ep 22/16-3 and Zi 368/4-3). We thank HASYLAB at DESY for generous allocation of beamtime and M. Knapp for experimental assistance.

References

Ahearn, G.A., Howarth, F.G., 1982. Physiology of cave arthropods in Hawaii. J. Exp. Zool. 222, 227–238.

Aizenberg, J., Lambert, G., Weiner, S., Addadi, L., 2002. Factors involved in the formation of amorphous and crystalline calcium carbonate: a study of an ascidian skeleton. Am. Chem. Soc. 124, 32–39.

Al-Swalmih, A., Li, C., Siegel, S., Fratzl, P., Paris, O., in press. On the stability of amorphous minerals in the lobster cuticle. Adv. Mater. Q4

Anderson, J.F., 1970. Metabolic rates of spiders. Comp. Biochem. Physiol. 33, 51–72.

Bachra, B.N., Trautz, O.R., Simon, S.L., 1963. Precipitation of calcium carbonates and phosphates: I. Spontaneous precipitation of calcium carbonates and phosphates under physiological conditions. Arch. Biochem. Biophys. 103, 124–138.

Becker, A., Bismayer, U., Epple, M., Fabritius, H., Hasse, B., Shi, J., Ziegler, A., 2003. Structural characterisation of X-ray amorphous calcium carbonate (ACC) in sternal deposits of the Crustacea *Porcellio scaber*. Dalton Trans. 2003, 551–555.

Becker, A., Ziegler, A., Epple, M., 2005. The mineral phase in the cuticles of two species of Crustacea consists of magnesium calcite, amorphous calcium carbonate, and amorphous calcium phosphate. Dalton Trans. 2005, 1814–1820.

Boßelmann, F., Romano, P., Fabritius, H., Raabe, D., Epple, M., 2007. The composition of the exoskeleton of two crustacea: the american lobster *Homarus americanus* and the edible crab *Cancer pagurus*. Thermochim. Acta 463, 65–68.

Bouligand, Y., 1972. Twisted fibrous arrangements in biological materials and cholesteric mesophases. Tissue Cell 4, 189–217.

Cammenga, H.K., Epple, M., 1995. Basic principles of thermoanalytical techniques and their applications in preparative chemistry. Angew. Chem. Int. Ed. 34, 1171–1187.

Coblentz, F.E., Shafer, T.H., Roer, R.D., 1998. Cuticular proteins from the blue crab alter in vitro calcium carbonate mineralization. Comp. Biochem. Physiol. B 121, 349–360.

Compère, P., 1990. Fine structure and elaboration of the epicuticle and the pore canal system in tergite cuticle of the land isopod *Oniscus asellus* during a moulting cycle. In: Juchault, P., Mocquard, J.P. (Eds.), The Biology of Terrestrial Isopods: III. Proceedings of the Third International Symposium on the Biology of Terrestrial Isopods. Université de Portiers, pp. 169–175.

Compère, P., 1995. Fine structure and morphogenesis of the sclerite epicuticle in the Atlantic shore crab *Carcinus maenas*. Tissue Cell 27, 525–538.

Compère, P., Goffinet, G., 1995. Cytochemical demonstration of acid mucoploysaccharides in the epicuticular surface coat of the crab *Carcinus Maenas* (L.) (Crustacea, Decapoda). Belg. J. Zool. 125, 95–100.

Christiansen, K., 2004. Adaptation: morphological (external). In: Gunn, J. (Ed.), Encyclopedia of Caves and Karst Science, pp. 7–9.

Dillaman, R., Hequembourg, S., Gay, M., 2005. Early pattern of calcification in the dorsal carapace of the blue crab, *Callinectes sapidus*. J. Morphol. 263, 356–374.

Fabritius, H., Ziegler, A., 2003. Analysis of $CaCO_3$ deposit formation and degradation during the molt cycle of the terrestrial isopod *Porcellio scaber* (Crustacea, Isopoda). J. Struct. Biol. 142, 281–291.

Fabritius, H., Walther, P., Ziegler, A., 2005. Architecture of the organic matrix in the sternal CaCO3 deposits of *Porcellio scaber* (Crustacea, Isopoda). J. Struct. Biol. 150, 190–199.

Galat, A., Popowicz, J., 1978. Study of the Raman scattering spectra of chitins. Biochemistry 26, 519–524.

Glötzner, J., Ziegler, A., 2000. Morphometric analysis of the plasma membranes in the calcium transporting sternal epithelium of the terrestrial isopods *Ligia oceanica*, *Ligidium hypnorum* and *Porcellio scaber*. Arthropod Struct. Dev. 29, 241–257.

Goldsmith, J.R., Graf, D.L., 1958. Relation between lattice constants and composition of the Ca–Mg carbonates. Am. Mineral. 43, 84–101.

Greenaway, P., 1985. Calcium balance and moulting in the crustacea. Biol. Rev. 60, 425–454.

Gualtieri, A., 2000. Accuracy of XRPD QPA using the combined Rietveld–RIR method. J. Appl. Crystallogr. 33, 267–278.

Hadley, N.F., Ahearn, G.A., Howarth, F.G., 1981. Water and metabolic relations of cave-adapted and epigean lycosid spiders in Hawaii. J. Arachnol. 9, 215–222.

Hadley, N.F., Warburg, M.R., 1986. Water loss in three species of xeric-adapted isopods: correlations with cuticular lipids. Comp. Biochem. Physiol. 85A, 669–672.

Hem, D.J., 1985. Study and Interpretation of the Chemical Characteristics of Natural Water. U.S. Geological Printing Office, Washington.

Hild, S., Marti, O., Ziegler, A., 2008. Spatial distribution of calcite and amorphous calcium carbonate in the cuticle of the terrestrial crustaceans *Porcellio scaber* and *Armadillidium vulgare*. J. Struct. Biol. 163, 100–108.

Hueppop, K., 1985. The role of metabolism in the evolution of cave animals. NSS Bull. 47, 136–146.

Knapp, M., Joco, V., Baehtz, C., Brecht, H.H., Berghaeuser, A., Ehrenberg, H., von Seggern, H., Fuess, H., 2004a. Position-sensitive detector system OBI for high resolution X-ray powder diffraction using on-site readable image plates. Nucl. Instrum. Meth. Phys. Res. A521, 565–570.

Knapp, M., Baehtz, C., Ehrenberg, H., Fuess, H., 2004b. The synchrotron powder diffractometer at beamline B2 at HASYLAB/DESY: status and capabilities. J. Synchrotron Radiat. 11, 328–334.

Lavoie, K.H., Helf, K.L., Poulson, T.L., 2007. The biology and ecology of north American cave crickets. J. Cave Karst Stud. 69, 114–134.

Levi-Kalisman, Y., Raz, S., Weiner, S., Addadi, L., Sagi, I., 2002. Structural differences between biogenic amorphous calcium carbonate phases using X-ray absorption spectroscopy. Adv. Funct. Mat. 12, 43–48.

Locke, M., 1966. The structure and formation of the cuticulin layer in the epicuticle of an insect, *Calpodes ethlius* (Lepidoptera, Hesperiidae). J. Morphol. 118, 461–494.

Loste, E., Wilson, M., Seshadri, R., Meldrum, F.C., 2003. The role of magnesium in stabilising amorphous calcium carbonate and controlling calcite morphologies. J. Cryst. Growth 254, 206–218.

Luquet, G., Marin, F., 2004. Biomineralisations in crustaceans: storage strategies. C. R. Palevol. 3, 515–534.

Mejía-Ortíz, L.M., López-Mejía, M., 2005. Are there adaptation levels to cave life in crayfish? J. Crustacean Biol. 25, 593–597.

Neues, F., Ziegler, A., Epple, M., 2007a. The composition of the mineralized cuticle in marine and terrestrial isopods: a comparative study. Cryst. Eng. Commun. 9, 1245–1251.

Neues, F., Ziegler, A., Epple, M., 2007b. The application of synchrotron radiation-based micro-computer tomography in biomineralization. In: Bäuerlein, E. (Ed.), Handbook of Biomineralization: The Biology of Biominerals Structure Formation, vol. 1. Wiley-VCH, pp. 369–380.

Price, J.B., Holdich, D.M., 1980. An ultrastructural study of the integument during the moult cycle of the woodlouse, *Oniscus asellus* (Crustacea, Isopoda). Zoomorphology 95, 250–263.

Reddy, M.M., 1977. Crystallization of calcium carbonate in the presence of trace concentrations of phosphorus-containing anions. J. Cryst. Growth 41, 287–295.

Rodriguez-Carvajal, J., 1990. FULLPROF: A Program for Rietveld Refinement and Pattern Matching Analysis. Abstracts of the Satellite Meeting on Powder Diffraction of the XV Congress of the IUCr, Toulouse, p. 127.

Roer, R., Dillaman, R., 1984. The structure and calcification of the crustacean cuticle. Am. Zool. 24, 893–909.

Rutt, H.N., Nicola, J.H., 1974. Raman spectra of carbonates of calcite structure. J. Physiol. C 7, 4522–4528.

Sauer, G.R., Zunic, W.B., Durig, J.R., Wuthier, R.E., 1994. Fourier transform Raman spectroscopy of synthetic and biological calcium phosphates. Calcif. Tissue Int. 54, 414–420.

Schmalfuss, H., 1984. Eco-morphological strategies in terrestrial isopods. Symp. Zool. Soc. Lond. 53, 49–63.

Schmidt, U., Hild, S., Ibach, W., Hollricher, O., 2005. Characterization of thin polymer films on the nanometer scale with confocal Raman AFM. Macromol. Symp. 230, 133–143.

Shafer, T.H., Roer, R.D., Midgette-Luther, C., Brookins, T.A., 1995. Postecdysial cuticle alteration in the blue crab, *Callinectes sapidus*: synchronous changes in glycoproteins and mineral nucleation. J. Exp. Zool. 271, 171–182.

Shechter, A., Berman, A., Singer, A., Freiman, A., Grinstein, M., Erez, J., Aflalo, E.D., Sagi, A., 2008a. Reciprocal changes in calcification of gastrolith and cuticle during the molt cycle of the red claw crayfish *Cherax quadricarcinus*. Biol. Bull. 214, 122–134.

Shechter, A., Glazer, L., Cheled, S., Mor, E., Weil, S., Berman, A., Bentov, S., Aflalo, E.D., Khalaila, I., Sagi, A., 2008b. A gastrolith protein serving a dual role in the formation of an amorphous mineral containing extracellular matrix. Proc. Natl. Acad. Sci. USA 105, 7129–7134.

Soejoko, D.S., Tjia, M.O., 2003. Infrared spectroscopy and X ray diffraction study on the morphological variations of carbonate and phosphate compounds in giant prawn (*Macrobrachium rosenbergii*) skeletons during its moulting period. J. Mater. Sci. 389, 2087–2093.

Štrus, J., Blejec, A., 2001. Microscopic anatomy of the integument and digestive system during the molt cycle in *Ligia italica* (Oniscidea). In: Kensley, B., Brusca, R.C. (Eds.), Isopod Systematics and Evolution. A.A. Balkema, Brookfield, pp. 343–352.

Sugawara, A., Nishimura, T., Yamamoto, Y., Inoue, H., Nagasawa, H., Kato, T., 2006. Self-organization of oriented calcium carbonate/polymer composites: effects of a matrix peptide isolated from the exoskeleton of a crayfish. Angew. Chem. Int. Ed. Engl. 45, 2876–2879.

Tlili, M.M., Ben Amor, M., Gabrielli, C., Joiret, S., Maurin, G., Rousseau, P., 2001. Characterization of $CaCO_3$ hydrates by micro-Raman spectroscopy. J. Raman Spectrosc. 33, 10–16.

Wheatly, M.G., 1999. Calcium homeostasis in crustacea: the evolving role of branchial, renal, digestive and hypodermal epithelia. J. Exp. Zool. 283, 620–640.

Wood, S., Russell, J.D., 1987. On the nature of the calcium carbonate in the exoskeleton of the woodlouse *Oniscus asellus* L. (Isopoda, Oniscoidea). Crustaceana 53, 49–53.

Yoder, J.A., Horton, H., Hobbs, I.I.I., Hazelton, M.C., 2002. Aggregate protection against dehydration in adult females of the cave cricket, *Hadenoecus cumberlandicus* (Orthoptera, Rhaphidophoridae). J. Cave Karst Stud. 64, 140–144.

Ziegler, A., 1997. Ultrastructural changes of the anterior and posterior sternal integument of the terrestrial isopod *Porcellio scaber* Latr. (Crustacea) during the moult cycle. Tissue Cell 29, 63–76.

Ziegler, A., 1994. Ultrastructure and electron spectroscopic diffraction analysis of the sternal calcium deposits of *Porcellio scaber* Latr. (Isopoda, Crustacea). J. Struct. Biol. 112, 110–116.

Ziegler, A., 2003. Variations of calcium deposition in terrestrial isopods. In: Sfenthourakis, S., De Araujo, P.B., Hornung, E., Schmalfuss, H., Taiti, S., Szlavecz, K. (Eds.), Crustaceana Monographs Edition. Koninklijke Brill NV, Leiden, pp. 299–309.

Ziegler, A., Fabritius, H., Hagedorn, M., 2005. Microscopical and functional aspects of calcium-transport and deposition in terrestrial isopods. Micron 36, 137–153.

Please cite this article in press as: Hild, S., et al. Ultrastructure and mineral distribution in the tergal cuticle of the terrestrial isopod *Titanethes albus*. Adaptations to a karst cave biotope. J. Struct. Biol. (2009), doi:10.1016/j.jsb.2009.07.017